

Observations of Tilt Instabilities in Field-Reversed Configurations of a Confined Plasma

M. Tuszewski, D. C. Barnes, R. E. Chrien, J. W. Cobb,^(a) D. J. Rej, R. E. Siemon, D. P. Taggart, and B. L. Wright

Los Alamos National Laboratory, Los Alamos, New Mexico 87545

(Received 13 August 1990)

We report the first consistent observations of internal tilt instabilities in field-reversed configurations. Detailed comparisons with numerical calculations establish that data from an array of external magnetic probes are signatures of these destructive plasma instabilities. As suggested by finite-Larmor-radius theory, field-reversed configurations appear grossly stable when s/e [(average number of ion gyroradii)/(separatrix elongation)] is less than 0.2–0.3 and show MHD-like tilt instabilities when $s/e \sim 1$.

PACS numbers: 52.35.Py, 52.55.Hc

A field-reversed configuration (FRC) is a confined plasma in the form of an elongated compact toroid with primarily poloidal magnetic fields.¹ FRCs are of interest because they offer an unusual fusion-reactor potential, including simple cylindrical geometry, ease of translation,² very high plasma β , and a natural divertor.¹ The latter two attributes make the FRC ideal for possible use of advanced fuels.³ However, the key issue in present FRC research is gross stability. An FRC equilibrium (see Fig. 1) consists of closed field lines with unfavorable curvature; it should be rapidly destroyed by an internal tilt instability⁴ according to the magnetohydrodynamic (MHD) model. Nevertheless, experiments to date have shown that FRCs can be grossly stable.^{1,5} Substantial kinetic effects (i.e., large ion gyroradii) may explain this apparent stability, but MHD-like FRCs will be required for possible fusion reactors.¹ This raises two important questions: (1) At what point do kinetic effects lose importance and MHD predictions of unstable behavior become applicable? (2) Will FRCs of interest for fusion remain grossly stable?

We report in this Letter the first clear observations of tilt instabilities in FRC experiments. Previous work revealed occasional FRC tiltlike motion, in particular, during plasma formation.^{5,6} The present tilt observations are made with an array of external magnetic pickup

loops, a new diagnostic in FRC research. Comparisons with 3D MHD simulations⁷ clearly identify features in the data with signatures of internal tilt instabilities. These results provide some answers to the above two questions: (1) The MHD model appears applicable as predicted by finite-Larmor-radius (FLR) theory,⁸ and (2) additional stabilizing techniques will be required for future large-size FRCs.

The data are obtained in the FRX-C/LSM field-reversed θ pinch⁹ sketched in Fig. 1. FRC formation starts by filling the quartz tube with deuterium gas (2–12.5 mtorr) and by applying a bias magnetic field (0.3–1.1 kG). The gas is ionized and the external field is suddenly reversed ($t=0$), which causes plasma radial compression. Field-line connection then occurs, with a good axial symmetry achieved by auxiliary end coils.⁹ Finally, the FRC contracts axially before reaching equilibrium. The diagnostics for these studies include diamagnetic loops, side-on interferometry, end-on visible and soft-x-ray cameras, and an array of 64 external B_θ pickup loops.¹⁰ The latter could detect instabilities as asymmetry-induced departures from the equilibrium condition, $B_\theta=0$. The noise level of this diagnostic is 1–2 G. Four $\pm z$ positions (z is the axial coordinate) shown in Fig. 1 allow separation of axially even and odd components. At each z location, eight loops at regular θ intervals (θ is the azimuthal angle) permit Fourier analysis for the $n \leq 3$ symmetries (n is the toroidal mode number).

FRCs with good confinement properties can be obtained in FRX-C/LSM, but only for bias fields less than 0.8–0.9 kG and for fill pressures less than 5 mtorr.⁹ For other initial conditions, poor FRC confinement is consistently observed.^{11,12} Many studies, to be reported elsewhere, have attempted to correlate this confinement degradation with some formation inadequacy, but they have proved inconclusive. Meanwhile, the B_θ probe array and end-on photos reveal several instabilities, including rotational modes,¹³ transient flutes,⁹ and tiltlike instabilities. Only the latter are strongly correlated with

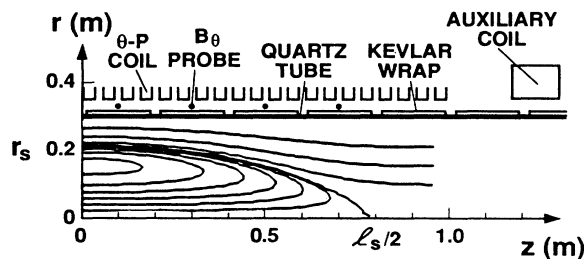


FIG. 1. Sketch of the FRX-C/LSM experiment. Flux contours are shown for a typical FRC equilibrium. There is axial symmetry about the coil midplane.

FRC confinement. Short diamagnetism decay times ($< 50 \mu\text{s}$) and large tilt amplitudes ($> 20 \text{ G}$) such as in Fig. 2 characterize poor FRCs, while large diamagnetism decay times ($\geq 200 \mu\text{s}$) and small tilt amplitudes ($\leq 5 \text{ G}$) characterize good FRCs. The tilt amplitudes discussed in this Letter are the $n=1$ Fourier amplitudes of the axially odd B_θ asymmetries.

The tilt data are compared with internal tilt instabilities in 3D MHD simulations.⁷ Fifteen 5-mtorr FRCs (0.7–1-kG bias fields) are considered that have similar plasma parameters at 15–20 μs . The separatrix radii and lengths are $r_s = 22 \pm 1 \text{ cm}$ and $l_s = 155 \pm 5 \text{ cm}$. The external fields are $4.3 \pm 0.1 \text{ kG}$, the average densities are $n = (1 \pm 0.1) \times 10^{15} \text{ cm}^{-3}$, and the total temperatures are $T_e + T_i = 340 \pm 40 \text{ eV}$. Electron temperatures $T_e = 140 \pm 15 \text{ eV}$ are measured for those conditions.¹² For the simulations, a 2D MHD equilibrium with similar parameters (shown in Fig. 1) is perturbed at $t=0$ by an axial velocity trial function¹⁴ of up to 1% of the Alfvén speed. This percentage provides good agreement on average between data and calculations. There are no other adjustable parameters. The calculations then show growing $n=1$ internal tilt instabilities. Higher-order modes are not considered in the simulations.

The results from two calculations with classical (dashed curves) and 100 times classical (dotted curves) plasma resistivities are shown in Fig. 2. These two cases should provide lower and upper bounds to the unknown experimental resistivities.^{11,12} The computations could not be carried beyond 38 μs with the particular end boundary conditions that were used. The measured and calculated diamagnetism are in agreement [Fig. 2(a)], except of course for the large peak at 7 μs due to axial dynamics during FRC formation. The axial dynamics

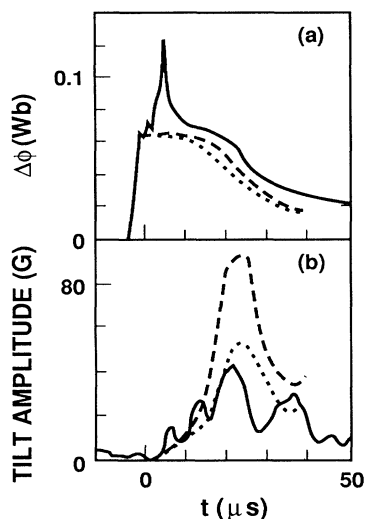


FIG. 2. Time histories of (a) midplane diamagnetism and (b) tilt amplitude at $z=0.1 \text{ m}$. Dashed and dotted lines are numerical results (see text) and solid lines are 5-mtorr data.

also coincide with the onset of oscillations in tilt amplitude as in Fig. 2(b). These oscillations are not observed in some 3-mtorr discharges where the tilt develops well after axial dynamics ($t > 50 \mu\text{s}$).

The time histories of data and calculations present many similarities. The observed tilt growth times are $5.3 \pm 0.8 \mu\text{s}$, the amplitudes peak at $23 \pm 4 \mu\text{s}$, and drop subsequently to 0.46 ± 0.17 of the peak values. These quantities are in good agreement with the calculated values, as seen in Fig. 2. The quoted experimental errors are standard deviations over the fifteen 5-mtorr discharges. However, more realistic error bars for the tilt growth times are 2–3 μs because of additional uncertainties associated with oscillations. The measured peak amplitudes of $35 \pm 10 \text{ G}$ are lower than the calculated values of 50–90 G. The latter depend on plasma resistivity as seen in Fig. 2, and could also be sensitive to plasma on open field lines since the B_θ asymmetries decrease by about a factor of 10 from just inside the separatrix up to the wall.

The simulations indicate that the FRC topology is approximately preserved before peak tilt amplitude. The latter occurs when the internal toroidal and poloidal fields become comparable. After the peak, field lines open up rapidly. This transition is illustrated in Fig. 3 with pressure contours at (a) 20 μs and (b) 30 μs from

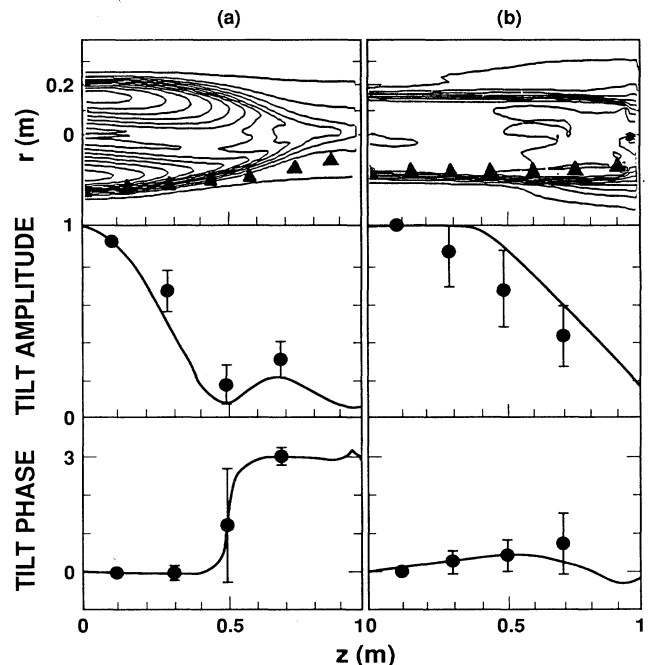


FIG. 3. Plasma pressure contours and axial profiles of the relative amplitude and azimuthal phase of the tilt component of B_θ , showing a transition from (a) closed (20 μs) to (b) open (30 μs) field-line configurations. The lines are numerical results, circles are 5-mtorr tilt data, and triangles are 5-mtorr excluded-flux-radius data.

the calculation with classical resistivity of Fig. 2. Averaged 5-mtorr data points are also shown in Fig. 3. The calculated and observed axial dependences are in very good agreement (the two calculations of Fig. 2 have similar axial dependences). They show in Fig. 3(a) a minimum amplitude and a π phase jump (relative to midplane values) near $z=0.5$ m where the tilt component of B_θ changes sign. The midplane phases vary from discharge to discharge, suggesting that the tilt does not grow from an external field error at fixed azimuthal angle. As seen in Fig. 3(b), the minimum in tilt amplitude and its associated π phase jump have moved out of the coil region by $30 \mu\text{s}$.

All diagnostics display sudden changes after peak tilt amplitude that are consistent with field-line opening. The diamagnetism drops at the midplane as seen in Fig. 2(a) and becomes axially flat as illustrated by the excluded flux radius¹ ($\sim \Delta\phi^{1/2}$) indicated by triangles in Fig. 3. The observed $\Delta\phi$ decay times ($\sim 80 \mu\text{s}$) after $30\text{--}40 \mu\text{s}$ are consistent with open field lines. Side-on interferometry shows a sudden transition from elliptical to flattened density profiles similar to that of the diamagnetism. Sudden density increases are observed outside of the coil soon after peak tilt amplitudes. Multiple-exposure end-on photos consistently show evidence of wall contact after peak tilt amplitude.

Data similar to those in Figs. 2 and 3 are also obtained at 2–4-mtorr fill pressures with bias fields around 1 kG. Higher plasma temperatures result in larger tilt growth rates and earlier peak amplitudes, as suggested by the MHD model [$\gamma_{\text{MHD}} \sim 2v_A/l_s$ with $v_A^2 = 2(T_e + T_i)/m_i$]. For example, 3-mtorr tilt amplitudes peak at $16 \pm 4 \mu\text{s}$ ($16 \mu\text{s}$ calculated with classical resistivity). Tilt asymmetries are also observed at fill pressures greater than 5 mtorr, but with an increasing proportion of $n=2$ and 3 axially even and odd components. All asymmetries tend to develop earlier and with smaller amplitudes as the fill pressure is increased. At 10 mtorr, asymmetries are observed from $2\text{--}3 \mu\text{s}$ and have amplitudes less than 10 G at all times. These collisional plasmas, which have relatively smooth $\Delta\phi$ decays and total lifetimes of $100\text{--}200 \mu\text{s}$, could be in the same class as the TRX-2 hydrogen discharges which gave no apparent sign of tilt instabilities.⁵

Two parameters appear to govern the growth of the FRC tilt instabilities. The first one¹⁴ is the ratio s of torus minor radius ($a \sim r_s/4$) to average internal ion gyroradius ($\rho_i = v_i/\Omega_{ci}$, with $v_i^2 = T_i/m_i$ and $\Omega_{ci} = e(B_i)/m_i$). In general, s increases with bias field (larger r_s) and fill pressure (smaller T_i). The second parameter is the FRC elongation $e = l_s/2r_s$. Its influence is suggested by applying FLR theory⁸ to the FRC tilt instability. Qualitatively, stabilization might be expected if $(k\rho_i)^2 \geq \gamma_{\text{MHD}}/\Omega_{ci}$, where $k \sim 1/r_s$ and $\gamma_{\text{MHD}}/\Omega_{ci} \sim 2\rho_i/l_s$. This inequality can be rewritten as $s/e \leq 1/4$. A similar condition is obtained for FLR flute stabilization in mirror machines and has been suggested for

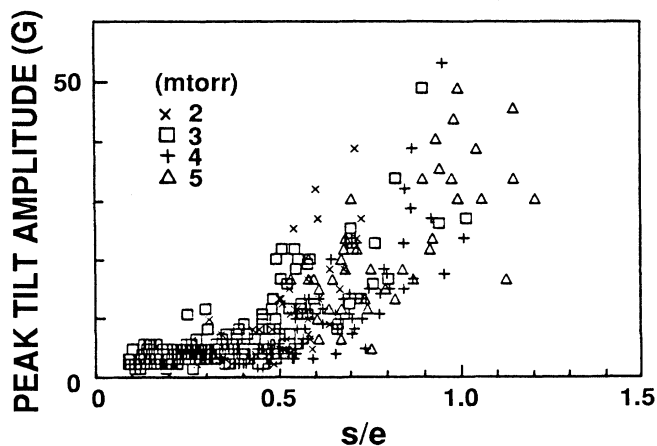


FIG. 4. Measured peak tilt amplitudes as functions of the stability parameter s/e [(average number of ion gyroradii)/(separatrix elongation)].

FRCs.¹⁵ A recent FLR calculation for FRCs also yields a quantitatively similar result.¹⁶

The peak tilt amplitudes of 340 discharges are shown in Fig. 4 as functions of s/e , where s ($\sim 1\text{--}5$) and e ($\sim 3\text{--}8$) are estimated at $15 \mu\text{s}$. For $s/e < 0.2\text{--}0.3$, consistently low peak amplitudes imply little or no tilt growth, which is consistent with the above FLR estimate. For $s/e \sim 0.8\text{--}1.2$, MHD-like tilt amplitudes, growth rates, time histories, and axial dependences (see Figs. 2 and 3) are also consistent with FLR theory. For $s/e \sim 0.3\text{--}0.7$, there seems to be a gradual transition between the two regimes just described, as found in Vlasov-fluid¹⁴ and Hall-fluid⁷ calculations. The details of this transition remain unknown because growth rates and axial dependences cannot be accurately determined for small amplitudes.

The correlation in Fig. 4 is the best found so far. In particular, tilt amplitudes do not scale as well with s alone. The significant scatter in Fig. 4 may be caused by differences in initial conditions or additional hidden stability parameters. However, we do not know a systematic effect other than the tilt that could generate the overall trend of Fig. 4. Other observations suggest a stabilizing influence of larger FRC elongations. Poor FRC confinement occurs whenever strong axial implosions during formation¹ result in short FRC lengths. Translated FRCs with $s \sim 1.5$ suddenly collapse when their elongations drop to around 2.

If tilt stability requires $s/e < 0.3$ while ignition may require¹ $s \sim 15\text{--}30$, FRC fusion reactors might be unattractively long. This illustrates the need for additional stabilizing techniques. Tilt stabilization is difficult⁷ but it has been recently demonstrated¹⁷ in the 3D simulation of Fig. 3 with the addition of a beam-ion component. The available technologies are now being considered to assess whether it is practical to inject an intense ion beam during FRC formation in present and in future

large-size FRC devices. The partial loss of fusion products may naturally produce some beam-ion component in ignited FRCs.³

In summary, the FRX-C/LSM data detailed in this Letter, particularly those from B_θ pickup loops, clearly show the signatures of FRC internal tilt instabilities indicated by 3D MHD simulations. These data are the first consistent observations of these destructive instabilities predicted by MHD theory. The data and FLR theory suggest apparent tilt stability for very kinetic and elongated FRCs, a regime in which most FRC experiments have operated until now. However, the MHD predictions of unstable behavior seem to be rapidly recovered when one departs from this regime. Additional stabilizing techniques will be required in future large-size FRCs.

The authors are grateful for excellent technical assistance on the FRX-C/LSM experiment. This work is supported by the U.S. Department of Energy.

^(a)Present address: Institute for Fusion Studies, University of Texas, Austin, TX 78712.

¹M. Tuszewski, Nucl. Fusion **28**, 2033 (1988).

²D. J. Rej *et al.*, Phys. Fluids **29**, 852 (1986).

³H. L. Berk, H. Momota, and T. Tajima, Phys. Fluids **30**, 3548 (1987).

⁴M. N. Rosenbluth and M. N. Bussac, Nucl. Fusion **19**, 489 (1979); J. H. Hammer, Nucl. Fusion **21**, 488 (1981).

⁵J. T. Slough and A. L. Hoffman, Nucl. Fusion **28**, 1121 (1988).

⁶J. T. Slough, A. L. Hoffman, and R. D. Milroy, Phys. Fluids B **1**, 840 (1989).

⁷R. D. Milroy *et al.*, Phys. Fluids B **1**, 1225 (1989).

⁸M. N. Rosenbluth, N. A. Krall, and N. Rostoker, Nucl. Fusion Suppl., Pt. 1, 143 (1962).

⁹R. E. Siemon *et al.*, in *Plasma Physics and Controlled Nuclear Fusion Research, 1988* (IAEA, Vienna, 1989), Vol. II, p. 517.

¹⁰M. Tuszewski, Rev. Sci. Instrum. **61**, 2937 (1990).

¹¹D. J. Rej *et al.*, Phys. Fluids B **2**, 1706 (1990).

¹²D. J. Rej *et al.*, Nucl. Fusion **30**, 1087 (1990).

¹³M. Tuszewski *et al.*, Phys. Fluids B **2**, 2541 (1990).

¹⁴D. C. Barnes *et al.*, Phys. Fluids **29**, 2616 (1986).

¹⁵D. V. Anderson *et al.*, in *Plasma Physics and Controlled Nuclear Fusion Research, 1980* (IAEA, Vienna, 1981), Vol. I, p. 469.

¹⁶L. C. Steinhauer and A. Ishida, Phys. Fluids B **2**, 2422 (1990).

¹⁷D. C. Barnes and R. D. Milroy (to be published).